Electronic Supplementary Material (ESI) for Journal of Materials Chemistry A.

Supporting Information

Choosing the right carbon additive is of vital importance for high-performance Sb-based Na-ion batteries

Kristina Pfeifer [a], Stefanie Arnold [a, b], Öznil Budak [b, c], Xianlin Luo [a], Volker Presser [b, c] Helmut Ehrenberg [a, d] and Sonia Dsoke*[a, d]

a Institute for Applied Materials (IAM), Karlsruhe Institute of Technology (KIT), Hermann-von-Helmholtz-Platz 1, 76344 Eggenstein-Leopoldshafen, Germany

b INM - Leibniz Institute for New Materials, 66123 Saarbrücken, Germany

c Department of Materials Science and Engineering, Saarland University, 66123 Saarbrücken, Germany

d Helmholtz-Institute Ulm for Electrochemical Energy Storage (HIU), P.O. Box 3640, 76021 Karlsruhe, Germany

* corresponding author's email: sonia.dsoke@kit.edu

1. Influence of FEC on the electrochemical performance of Na-metal containing half-cells

In our previous work, we were highlighting the importance of an appropriate half-cell setup for sodium-ion batteries.[1] The reactivity of sodium towards carbonate-based electrolytes can cause a degradation of the electrochemical system. It was reported that the addition of FEC could stabilize Na metal in carbonate-based electrolytes forming a protective polymer layer on the surface of the metal.[2,3,4] Therefore, the previously reported optical analysis[1] was repeated with addition of 5 % FEC to the 1 M $NaClO_4$ in EC/DMC electrolyte. Additionally, electrochemical cycling of an Sb/C65 electrode containing 70 mass% Sb, 20 mass% C65 and 10 mass% carboxymethyl cellulose (CMC) was performed utilizing the electrolyte with and without FEC additive.

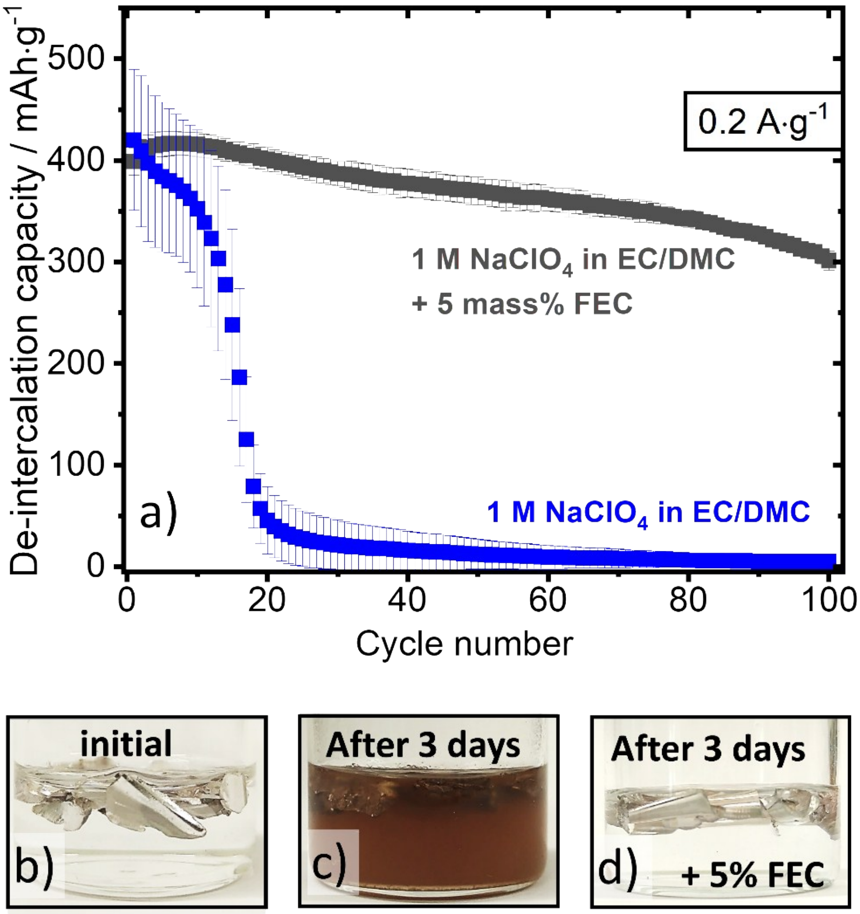

Figure S1 **a) electrochemical cycling stability of Sb/C65 in E-$NaClO_4$ and E-$NaClO_4$-FEC; b) Na metal the electrolyte right after Na addition (representative for both electrolytes); c) Na metal in 1 M $NaClO_4$ in EC/DMC after three days; d) Na metal in 1 M $NaClO_4$ in EC/DMC + 5 mass% FEC after three days.**

Figure S1a reveals that the addition of FEC leads to a stable cycling behavior of Sb/C65. In contrast, the absence of this additive causes a massive instability of the Sb/C65 half-cell. A possible explanation can be given by a correlation of this result to **Figure 1b-d**. The sodium metal has a shiny metallic surface right after addition to the clear liquid electrolyte (**Figure S1b**). This visual appearance does not change after three days in 1M $NaClO_4$ in EC/DMC + 5 mass% FEC (**Figure S1d**). On the contrary, a drastic color change of FEC free electrolyte can be observed and is deeply discussed in Ref. [1]. Most probably, FEC does not only improve the SEI properties of the Sb based working electrode as proposed in state-of-the-art literature,[3–5] but massively contributes to the protection of sodium against side reactions with the electrolyte.[6] As FEC suppresses the reactivity of sodium towards the electrolyte, metallic sodium counter and reference electrodes do not need to be replaced in a three-electrode half-cell setup. For this reason, an FEC containing electrolyte will be used for further experiments.

Table S1. Values obtained from gas sorption analysis of the different carbon samples.

Sample	**QSDFT surface area / $m^2 \cdot g^{-1}$**	**BET surface area / $m^2 \cdot g^{-1}$**	**Total pore volume /$cm^3 \cdot g^{-1}$**	**Micropore volume / $cm^3 \cdot g^{-1}$**	**Average pore width / nm**
C65	54	64	0.12	0.01	9.7
KS6L	21	24	0.05	0.01	10.1
Nanostars	293	395	0.71	0.12	15.3
OLC1300V	286	314	1.06	0.05	12.9
OLC1700A	205	223	0.57	0.04	11.1
SuperP	55	62	0.11	0.01	9.9

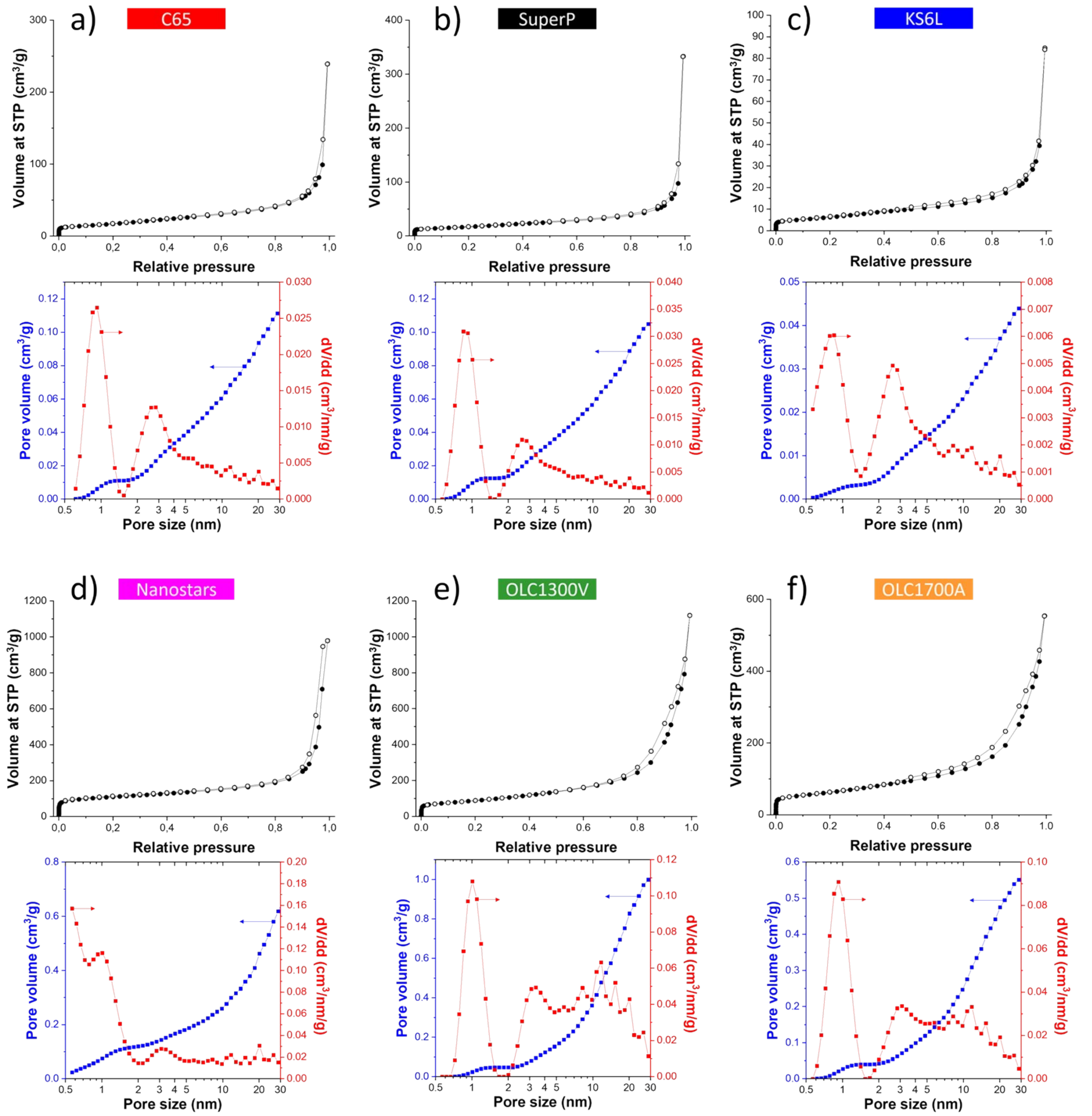

Figure S2 Gas sorption isotherms and pore volume distributions of a) C65, b) SuperP, c) KS6L, d) nanostars, e) OLC1300V, and f) OLC1700A.

Table S2. Values obtained from Raman analysis of the different carbons.

Sample	D-mode position / cm^{-1}	D-mode FWHM / cm^{-1}	G-mode position / cm^{-1}	G-mode FWHM / cm^{-1}	I_D/I_G ratio
C65	1347±2	128±5	1593±3	80±4	2.3±0.4
C-Nergy KS6L	1353±1	43±2	1581±1	19±1	0.2±0.1
Nanostars	1333±2	58±3	1586±3	58±3	1.4±0.2
OLC1300V	1342±1	152±11	1590±1	80±4	3.1±0.8
OLC1700A	1344±1	60±2	1589±1	60±4	1.2±0.1
SuperP	1352±2	123±5	1603±2	76±4	2.6±0.4

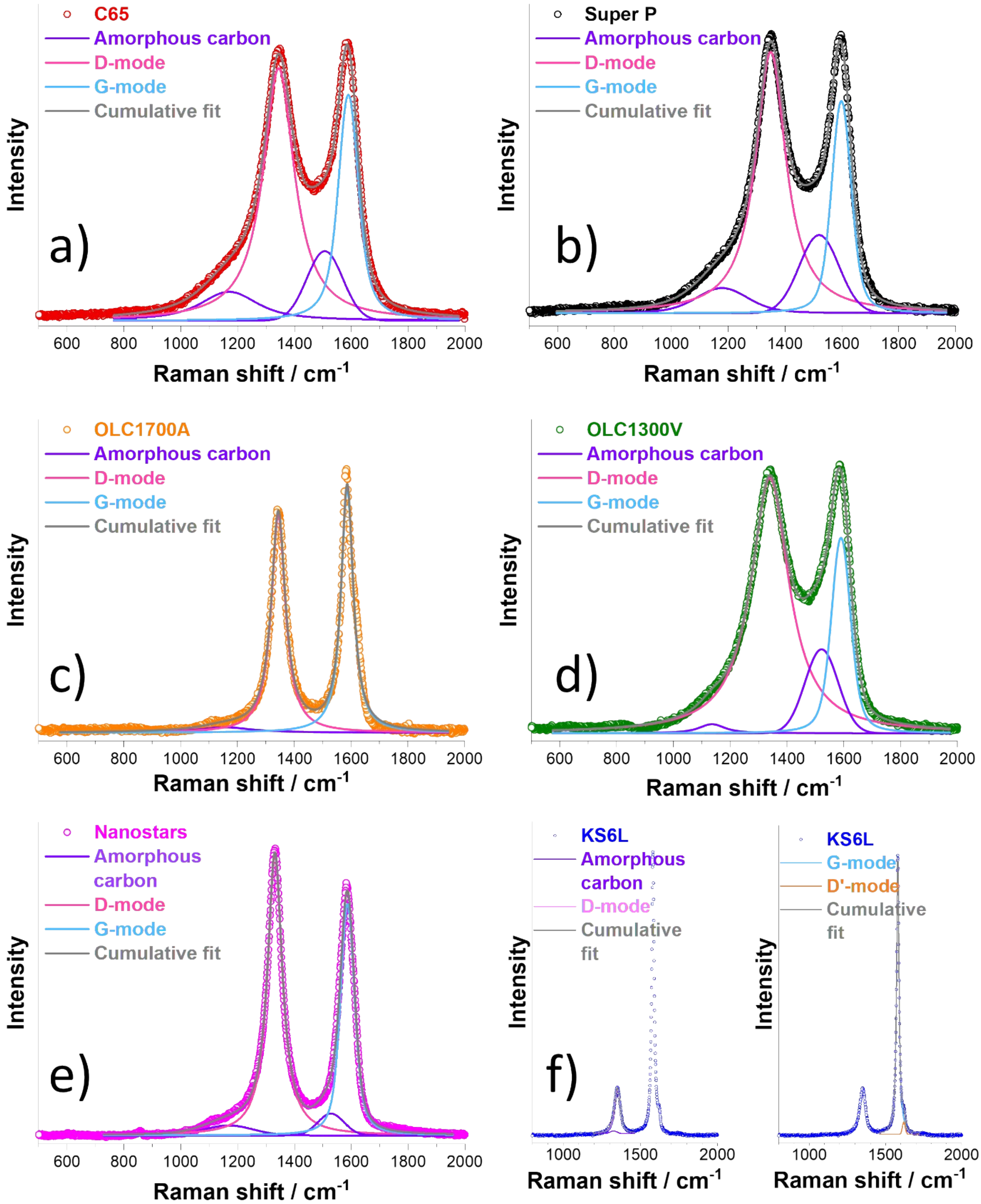

Figure S3 Measured and fitted Raman spectra of a) C65, b) SuperP, c) OLC1700A, d) OLC1300V, e) nanostars, and f) KS6L.

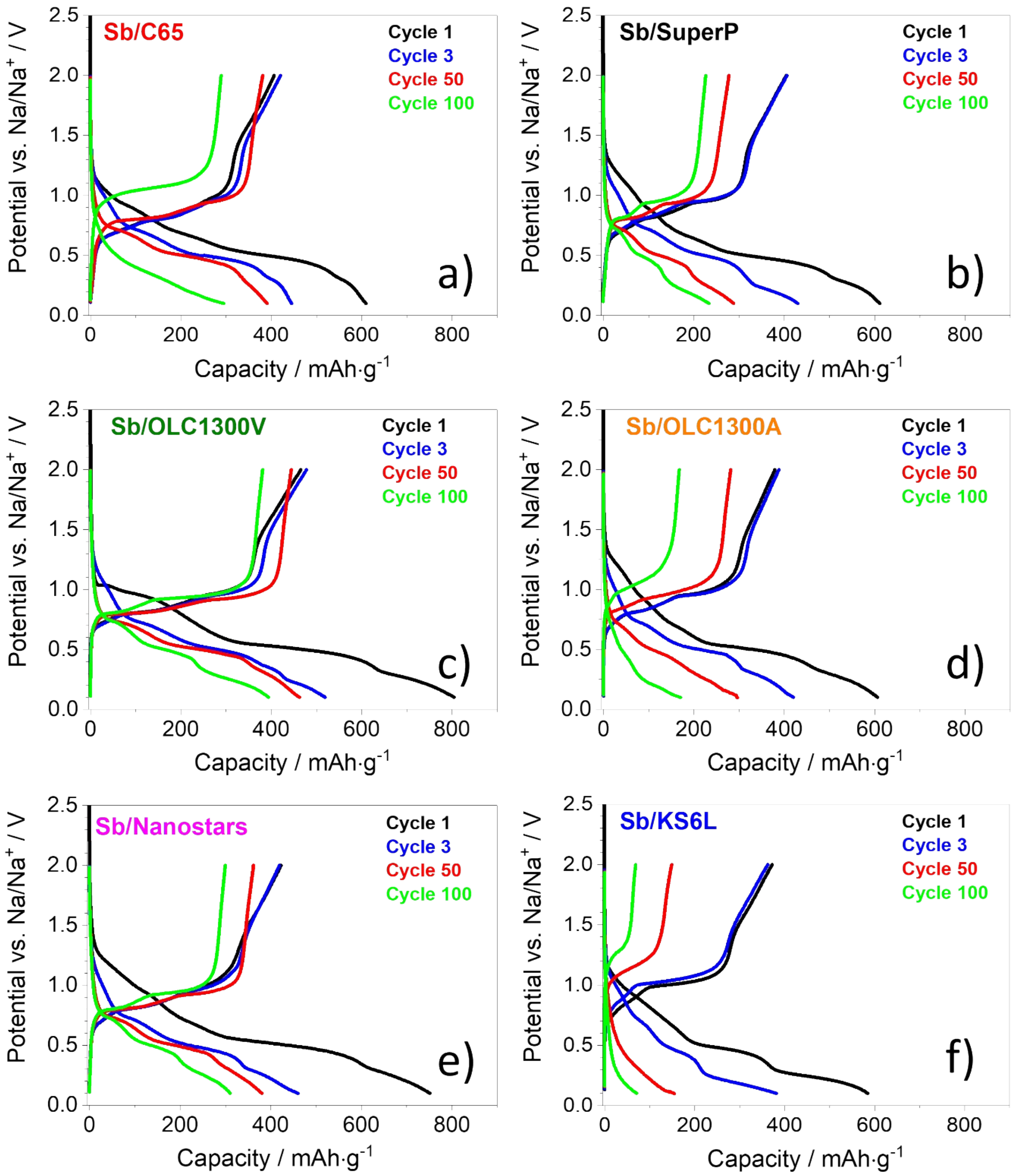

Figure S4 Galvanostatic charge/discharge profiles at 0.2 A·g^{-1} for a) Sb/C65, b) Sb/SuperP, c) Sb/OLC1300V, d) Sb/OLC1700A, e) Sb/nanostars, and f) Sn/KS6L.

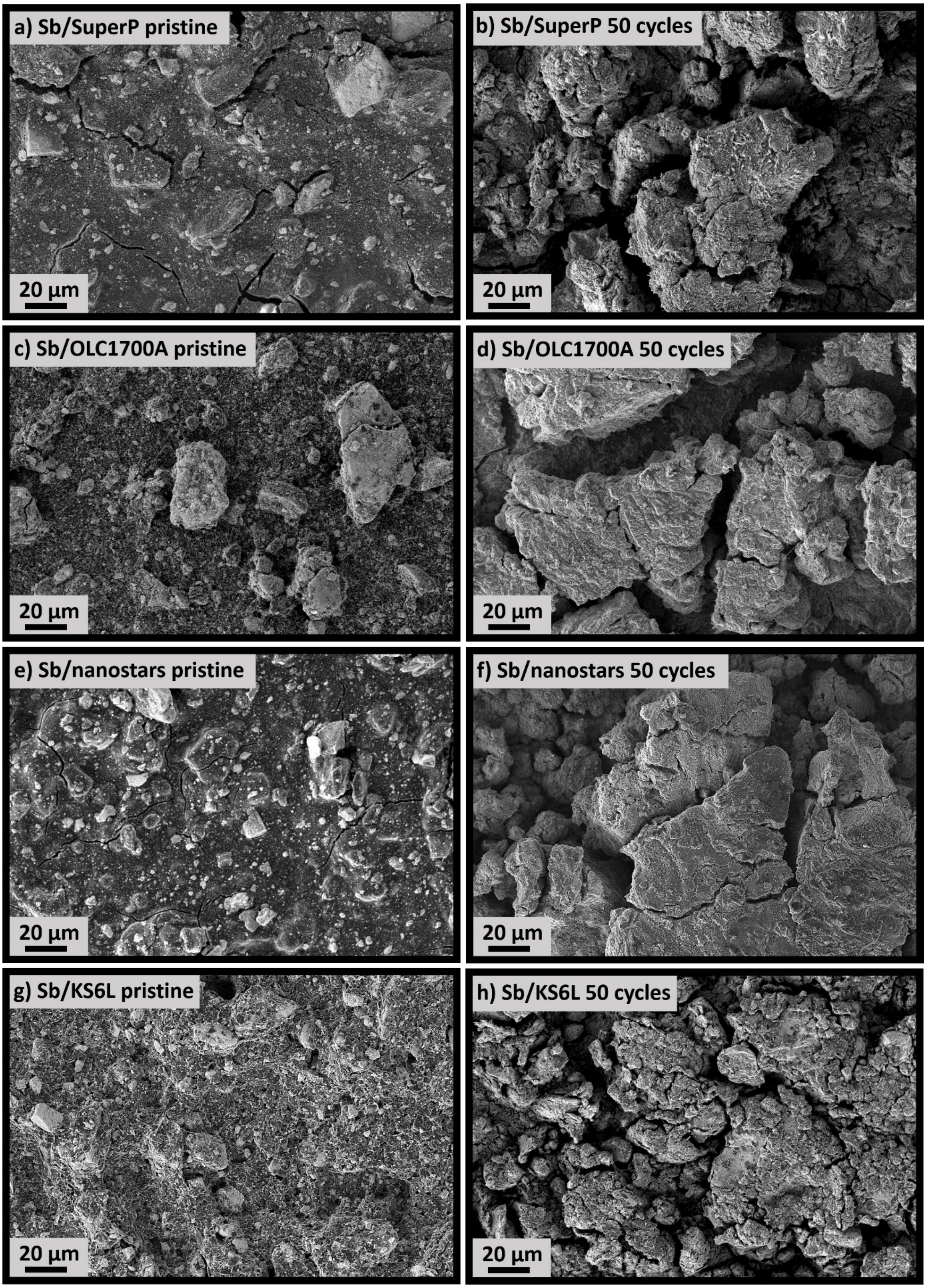

Figure S5 Scanning electron micrographs of a) pristine Sb/SuperP, b) Sb/SuperP after 50 cycles, c) pristine Sb/OLC1700A, d) Sb/OLC1700A after 50 cycles, e) pristine Sb/nanostars, f) Sb/nanostars after 50 cycles, g) pristine Sb/KS6L, and h) Sb/KS6L after 50 cycles.

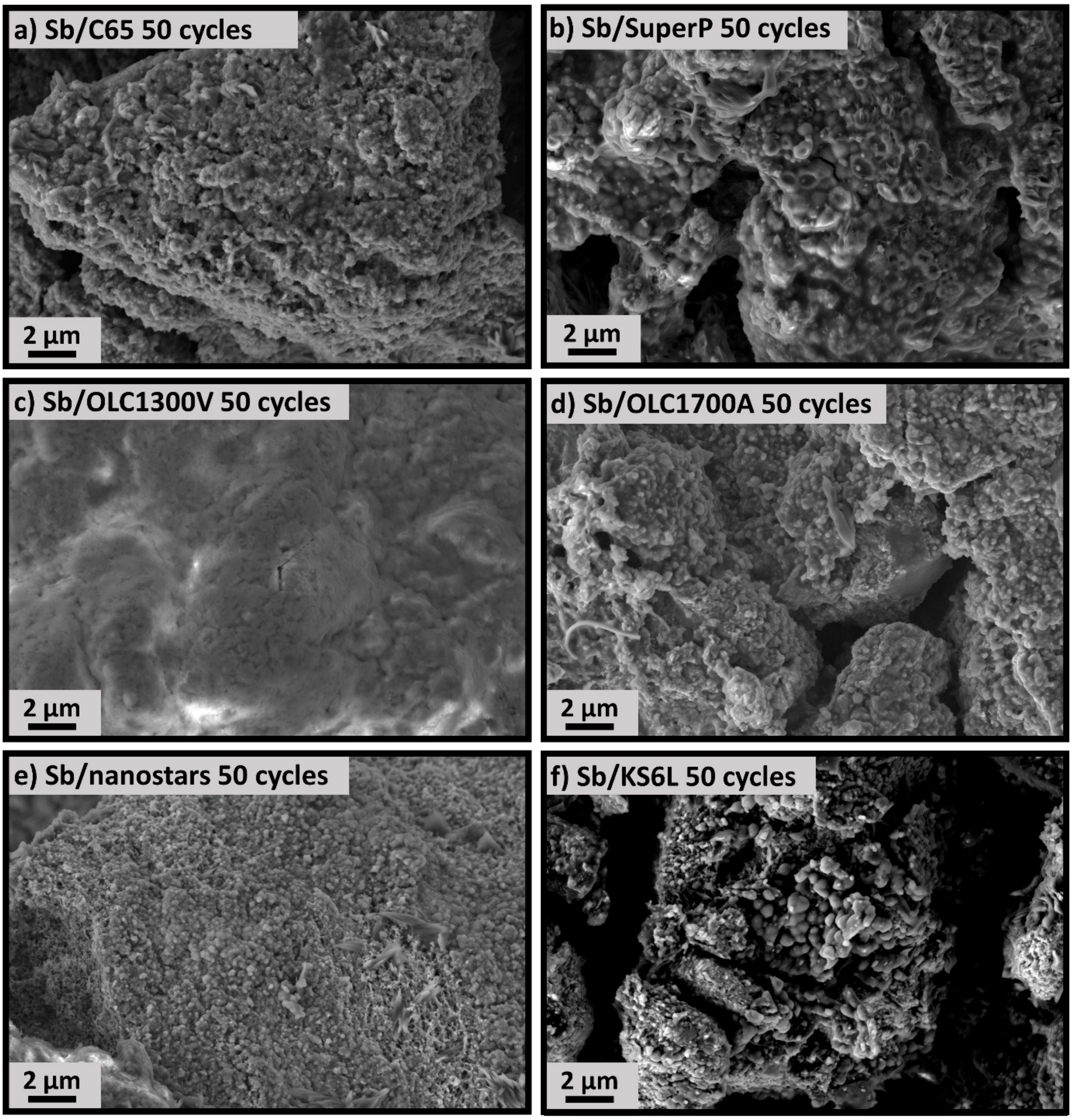

Figure S6 Scanning electron micrographs of a) Sb/C65, b) Sb/SuperP, c) Sb/OLC1300V, d) Sb/OLC1700A, e) Sb/nanostars, and f) Sb/KS6L after 50 cycles.

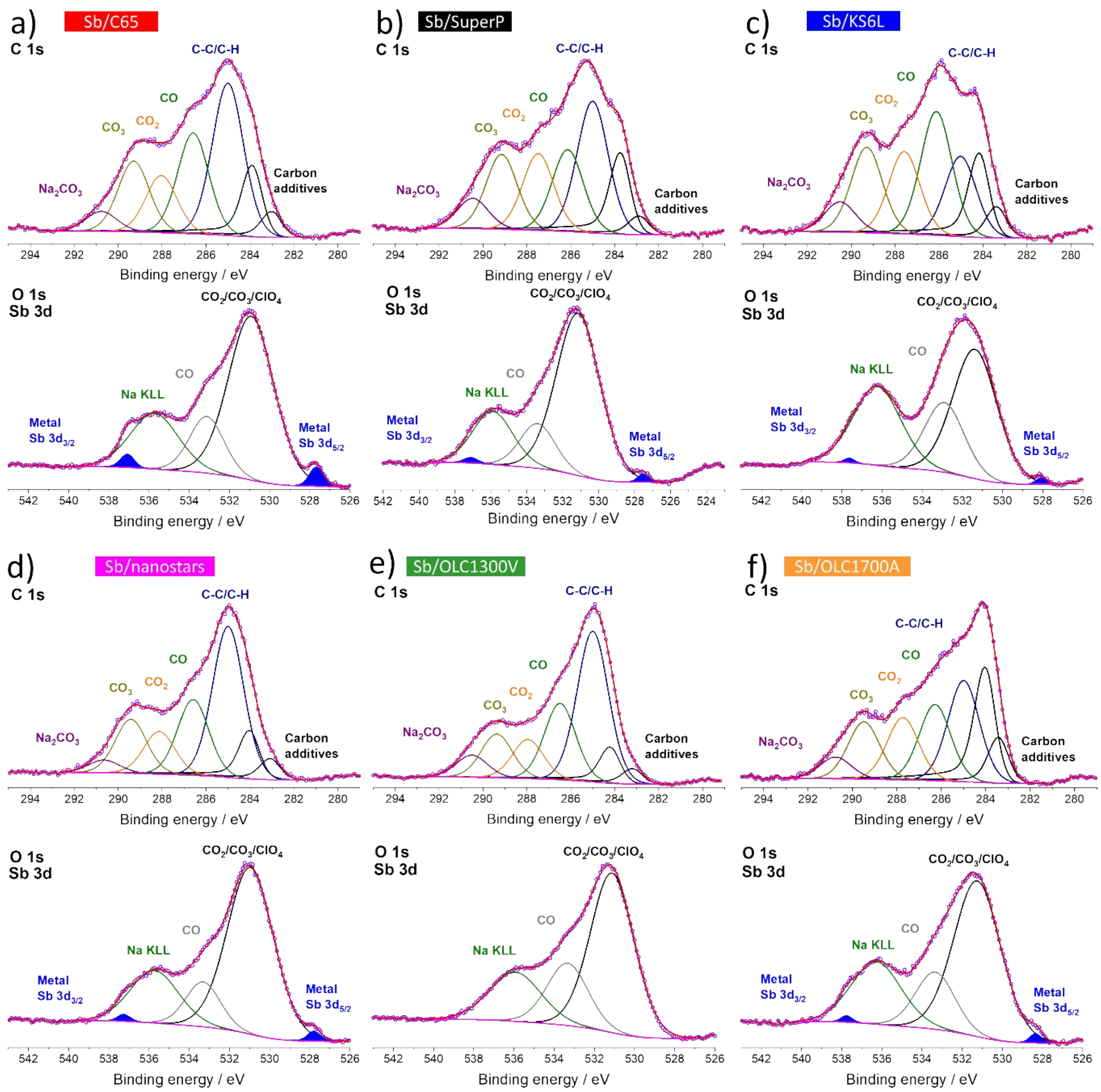

Figure S7 C 1s, O 1s and Sb 3d XPS spectra of a) Sb/C65, b) Sb/SuperP, c) Sb/KS6L, d) Sb/nanostars, e) Sb/OLC1300V, and f) Sb/OLC1700A after 50 cycles.

References

1 K. Pfeifer, S. Arnold, J. Becherer, C. Das, J. Maibach, H. Ehrenberg and S. Dsoke, *ChemSusChem*, 2019, **12**, 3312–3319.

2 a) R. Dugas, A. Ponrouch, G. Gachot, R. David, M. R. Palacin, J. M. Tarascon, *J. Electrochem. Soc.*, 2016, A2333-A3339; b) S. S. Zhang, *Journal of Power Sources*, 2006, **162**, 1379–1394; c) A. Darwiche, L. Bodenes, L. Madec, L. Monconduit and H. Martinez, *Electrochimica Acta*, 2016, **207**, 284–292;

3 A. Darwiche, C. Marino, M. T. Sougrati, B. Fraisse, L. Stievano and L. Monconduit, *Journal of the American Chemical Society*, 2012, **134**, 20805–20811.

4 J. Qian, Y. Chen, L. Wu, Y. Cao, X. Ai and H. Yang, *Chemical communications (Cambridge, England)*, 2012, **48**, 7070–7072.

5 H. Lu, L. Wu, L. Xiao, X. Ai, H. Yang and Y. Cao, *Electrochimica Acta*, 2016, **190**, 402–408.

6 Y. Lee, J. Lee, J. Lee, K. Kim, A. Cha, S. Kang, T. Wi, S. J. Kang, H.-W. Lee and N.-S. Choi, *ACS applied materials & interfaces*, 2018, **10**, 15270–15280.